

AN OPTIMIZATION APPROACH FOR THE DELAMINATION OF A COMPOSITE MATERIAL WITH NON-PENETRATION

M. HINTERMÜLLER*, V.A. KOVTUNENKO \diamond , AND K. KUNISCH*

ABSTRACT. A constrained variational problem for a composite with an interface crack subject to non-penetration conditions is considered. The composite consisting of two homogeneous orthotropic materials is described with respect to an in-plane deformation. The model is spatial, and we do not assume that it can be split into independent in-plane and anti-plane states. Based on the above model, we then describe a quasi-static delamination of the composite with a crack following the Griffith fracture criterion. This leads to a time-evolution problem for the (global) optimization of the total potential energy with respect to the crack length. Using a semi-smooth Newton algorithm, numerical experiments for an interface crack under mode-3 loading are presented and analyzed with respect to the half-angle β characterizing the coupling.

1. INTRODUCTION

A mathematical formulation of crack problems can be given within the framework of elasticity theory [20]. To gain some insight into the 3-dimensional situation, the standard approach is to simplify the elasticity model by splitting it into two 2-dimensional in-plane and anti-plane models. This, however, leads to a loss of information concerning the 3-dimensional nature of the system. Motivated by this drawback, we introduce an intermediate 2.5-dimensional model instead of the splitting approach. Our model is a spatial one since it takes into account all 3 components of the displacement vector, and still it is formulated in a 2-dimensional domain.

1991 *Mathematics Subject Classification.* 49J40, 49M29, 74M05, 74R10.

Key words and phrases. Composite material, interface crack, delamination, variational methods, semi-smooth Newton methods, constrained optimization.

* Department of Mathematics and Scientific Computing, University of Graz, Graz, Austria.

\diamond Lavrent'ev Institute of Hydrodynamics, Novosibirsk, Russia.

M.H. acknowledges support by Rice University, Dept. of Comput. and Appl. Math, Houston, Texas, USA, where part of the research was performed.

For the construction of the 2.5-dimensional model we consider a homogeneous orthotropic material with a vertical plane of elastic symmetry rotated with an angle β to a reference coordinate system. We compose two pieces of such a material along the interface given by the plane $x_2 = 0$ such that the corresponding angles in the upper and lower half-spaces are β and $-\beta$, respectively. For the formulation of elasticity models in composite laminates see [21]. We further assume that a crack is situated on part of the interface. Applying the assumption of plain deformation at $x_3 = \text{const}$, then due to the rotation, this results in a spatial model.

In our numerical experiments we observe 3-dimensional effects: mixing of crack modes (mode-1 with mode-3), and contact between opposite crack surfaces. They occur under pure mode-3 loading, which is ruled out for the in-plane and anti-plane models. Due to the latter phenomenon we are required to consider (unilaterally) constrained crack problems with non-penetration conditions as suggested in [12, 13]. The corresponding variational formulation provides the appropriate state space for the crack problem which has a singularity at the crack tip.

We investigate the geometric and physical features of the composite model by numerical experiments. For this purpose a semi-smooth Newton technique is adapted to constrained crack problems. Under suitable assumptions, semi-smoothness concepts will allow a locally super-linear convergence rate of the Newton iterates. For the problems under consideration semi-smooth Newton methods are equivalent to primal-dual active-set algorithms [7, 11]. They are an efficient tool for the numerical treatment of constrained variational problems. In numerical experiments, global and monotone convergence was observed, which is supported by the *a posteriori* analysis in [8]. For a class of variational problems subject to boundary-constraints, in [9] we applied an argument based on perturbation of M-matrices guaranteeing these convergence properties. Returning to the continuous setting of the problem, a penalization technique was utilized in [10] to obtain an approximate Lagrange multiplier, which enjoys extra L^p -regularity. For the numerical treatment of curvilinear cracks we refer to [19, 23], where extended finite element techniques are used.

One of the principal questions in fracture mechanics and structure design is to describe the stability properties of a solid with a crack and to predict its growth. By the Griffith fracture hypothesis the propagation of a crack is determined by the energy release rate at the crack tip, which cannot exceed a given physical parameter (see [3, 22]). A large number of papers investigated quasi-static growth of cracks in elastic media; see, e.g., [20, 6, 1, 16]. We argue that the energy release rate

is the shape derivative of the potential energy functional with respect to variations of the crack tip. In [12, 13] methods of shape sensitivity analysis were adopted to crack problems with non-penetration conditions to provide a formula for the shape derivative. This includes the Griffith formula as a specific case.

We observe that the Griffith fracture criterion provides a necessary optimality condition for a local minimum (if it exists) of the total potential energy, which is defined as the sum of the potential and the surface energy. On the other hand, global optimization problems require minimization over all admissible crack shapes (see [5, 2]). For strictly convex cost functionals these two concepts coincide. In fracture mechanics this corresponds to stable crack propagation (progressive). The case of unstable (or brutal) crack growth is related to non-convex cost functionals. It was noticed in [5] that for brutal growth the Griffith fracture law (as a local criterion) predicts a critical loading for the initiation of crack propagation larger than that needed by the global optimization approach. This fact is observed in our numerical tests, too. By the global formulation of the optimization problem, not only continuous solutions for the stable crack propagation but also solutions with jumps and discontinuous velocities of the propagation are obtained.

Well-posedness properties for time-evolution problems with cracks were analyzed in [4, 5]. In the present work we apply the global formulation of the optimization problem to a rectilinear crack and utilize it on a set of critical points derived in a constructive way from the Griffith fracture law. Note that the delamination process suggests a pre-defined path (along the interface) of the crack time-evolutions, which was confirmed experimentally [14]. This problem is solved numerically to describe the delamination of composite materials with an interface crack under quasi-static linear loading.

2. CONSTRAINED CRACK PROBLEMS FOR A COMPOSITE

In this section we formulate a model with respect to an in-plane deformation for two identical homogeneous orthotropic materials, which are composed at a planar interface with the angle of 2β between their vertical planes of elastic symmetry and which have a crack along a part of their interface.

2.1. Modelling of composite materials in plane deformation.

Consider a homogeneous orthotropic material with planes of elastic symmetry corresponding to the (x'_1, x'_2, x'_3) -axes. First, we compose the identical materials with respect to a reference coordinate system

(x_1, x_2, x_3) in the following way. In the "upper" half-space $\mathbb{R}_+^3 = \{x_1, x_2 \geq 0, x_3\}$ the (x'_1, x'_2, x'_3) -axes are rotated in the anti-clockwise direction to (x_1, x_2, x_3) with respect to the common $x'_2 = x_2$ -axis by the angle β between x'_3 and x_3 . The angle $\beta \in [-\pi/2, \pi/2]$ is arbitrarily fixed. In the "lower" half-space $\mathbb{R}_-^3 = \{x_1, x_2 \leq 0, x_3\}$ the (x'_1, x'_2, x'_3) -axes are rotated to (x_1, x_2, x_3) with respect to $x'_2 = x_2$ in the opposite direction by the same angle. The materials are assumed to be joined along the plane $x_2 = 0$.

For a displacement vector $u = (u_1, u_2, u_3)^\top(x)$ (at a point $x = (x_1, x_2, x_3)^\top \in \mathbb{R}^3$) in the composite material

$$u = u^+ \quad \text{in } \mathbb{R}_+^3, \quad u = u^- \quad \text{in } \mathbb{R}_-^3,$$

we introduce a strain tensor $\varepsilon = \{\varepsilon_{ij}\}$ according to the linear Cauchy law and a 3×3 symmetric tensor of stress $\sigma = \{\sigma_{ij}\}$ as

$$(2.1) \quad \sigma(u) = \sigma^\beta(u^+) \quad \text{in } \mathbb{R}_+^3, \quad \sigma(u) = \sigma^{-\beta}(u^-) \quad \text{in } \mathbb{R}_-^3.$$

Here and throughout we utilize the standard tensor notation common in linear elasticity and the summation convention for the repeated indices $i, j = 1, 2, 3$.

Second, we apply the assumption of plane deformation at every cross-section $x_3 = \text{const}$, which means that all three components of the displacement vector u do not depend on x_3 . Hence $\varepsilon_{33} = 0$ and the strain tensor takes the particular form

$$(2.2) \quad \begin{aligned} \varepsilon_{11}(u) &= u_{1,1}, & \varepsilon_{22}(u) &= u_{2,2}, & \varepsilon_{12}(u) &= 0.5(u_{1,2} + u_{2,1}), \\ \varepsilon_{13}(u) &= 0.5u_{3,1}, & \varepsilon_{23}(u) &= 0.5u_{3,2}. \end{aligned}$$

In \mathbb{R}_+^3 , the relevant components of the stress tensor (2.1) satisfy the following constitutive relations involving a non-symmetric matrix:

$$(2.3) \quad \begin{bmatrix} \sigma_{11}^\beta \\ \sigma_{22}^\beta \\ \sigma_{12}^\beta \\ \sigma_{23}^\beta \\ \sigma_{13}^\beta \end{bmatrix} = \begin{bmatrix} C_{11}^\beta & C_{12}^\beta & 0 & 0 & 2C_{16}^\beta \\ C_{12}^\beta & C_{22}^\beta & 0 & 0 & 2C_{26}^\beta \\ 0 & 0 & 2C_{44}^\beta & 2C_{45}^\beta & 0 \\ 0 & 0 & 2C_{45}^\beta & 2C_{55}^\beta & 0 \\ C_{16}^\beta & C_{26}^\beta & 0 & 0 & 2C_{66}^\beta \end{bmatrix} \begin{bmatrix} \varepsilon_{11} \\ \varepsilon_{22} \\ \varepsilon_{12} \\ \varepsilon_{23} \\ \varepsilon_{13} \end{bmatrix}$$

where 9 elasticity coefficients depending on β (except for C_{22}) have the form (see [18]):

$$\begin{aligned}
C_{11}^\beta &= C'_{33} \sin^4 \beta + 2(C'_{13} + 2C'_{66}) \sin^2 \beta \cos^2 \beta + C'_{11} \cos^4 \beta, \\
C_{66}^\beta &= C'_{66} + (C'_{33} + C'_{11} - 2C'_{13} - 4C'_{66}) \sin^2 \beta \cos^2 \beta, \\
C_{16}^\beta &= [C'_{11} \cos^2 \beta - C'_{33} \sin^2 \beta - (C'_{13} + 2C'_{66})(\cos^2 \beta - \sin^2 \beta)] \\
&\quad \times \sin \beta \cos \beta, \\
C_{44}^\beta &= C'_{44} \cos^2 \beta + C'_{55} \sin^2 \beta, \\
C_{55}^\beta &= C'_{44} \sin^2 \beta + C'_{55} \cos^2 \beta, \\
C_{45}^\beta &= (C'_{44} - C'_{55}) \sin \beta \cos \beta, \\
C_{12}^\beta &= C'_{23} \sin^2 \beta + C'_{12} \cos^2 \beta, \\
C_{26}^\beta &= (C'_{12} - C'_{23}) \sin \beta \cos \beta, \\
C_{22} &= C'_{22}.
\end{aligned}
\tag{2.4}$$

The coefficients subscribed with "prime" are related to the rotated coordinate system (x'_1, x'_2, x'_3) :

$$\begin{aligned}
C'_{11} &= \theta \left(\frac{1}{E_2} - \frac{\nu_{32}^2}{E_3} \right), & C'_{12} &= \theta \left(\frac{\nu_{21}}{E_2} + \frac{\nu_{31}\nu_{32}}{E_3} \right), \\
C'_{13} &= \theta \left(\frac{\nu_{31} + \nu_{21}\nu_{32}}{E_2} \right), & C'_{22} &= \theta \left(\frac{1}{E_1} - \frac{\nu_{31}^2}{E_3} \right), \\
C'_{23} &= \theta \left(\frac{\nu_{32}}{E_1} + \frac{\nu_{21}\nu_{31}}{E_2} \right), & C'_{33} &= \theta \frac{E_3}{E_2} \left(\frac{1}{E_1} - \frac{\nu_{21}^2}{E_2} \right), \\
C'_{44} &= G_{21}, & C'_{55} &= G_{32}, & C'_{66} &= G_{31}, \\
\frac{1}{\theta} &= \left(\frac{1}{E_2} - \frac{\nu_{32}^2}{E_3} \right) \left(\frac{1}{E_1} - \frac{\nu_{31}^2}{E_3} \right) - \left(\frac{\nu_{21}}{E_2} + \frac{\nu_{31}\nu_{32}}{E_3} \right)^2,
\end{aligned}
\tag{2.5}$$

with the material parameters

$$E_1, E_2, E_3, \nu_{21}, \nu_{32}, \nu_{31}, G_{21}, G_{32}, G_{31}.$$

The elasticity coefficients obey the following symmetry properties:

$$\begin{aligned}
C_{11}^{-\beta} &= C_{11}^\beta, & C_{12}^{-\beta} &= C_{12}^\beta, & C_{44}^{-\beta} &= C_{44}^\beta, & C_{55}^{-\beta} &= C_{55}^\beta, & C_{66}^{-\beta} &= C_{66}^\beta, \\
C_{16}^{-\beta} &= -C_{16}^\beta, & C_{26}^{-\beta} &= -C_{26}^\beta, & C_{45}^{-\beta} &= -C_{45}^\beta.
\end{aligned}
\tag{2.6}$$

Note that if $\beta = 0$ or $\beta = \pm\pi/2$ then we have $C_{16}^\beta = C_{26}^\beta = C_{45}^\beta = 0$ and (2.2), (2.3) are split into two independent states, namely the in-plane state for $(u_1, u_2)^\top$ and the anti-plane state for u_3 . If $\beta \neq 0, \pm\pi/2$ then we have a spatial model.

The substitution of (2.2) into (2.3) allows us to rewrite the constitutive law in the symmetric form:

$$\begin{aligned}
(2.7) \quad \sigma_{11}^\beta(u) &= C_{11}^\beta u_{1,1} + C_{12}^\beta u_{2,2} + C_{16}^\beta u_{3,1}, \\
\sigma_{22}^\beta(u) &= C_{12}^\beta u_{1,1} + C_{22}^\beta u_{2,2} + C_{26}^\beta u_{3,1}, \\
\sigma_{12}^\beta(u) &= C_{44}^\beta (u_{1,2} + u_{2,1}) + C_{45}^\beta u_{3,2}, \\
\sigma_{23}^\beta(u) &= C_{45}^\beta (u_{1,2} + u_{2,1}) + C_{55}^\beta u_{3,2}, \\
\sigma_{13}^\beta(u) &= C_{16}^\beta u_{1,1} + C_{26}^\beta u_{2,2} + C_{66}^\beta u_{3,1}.
\end{aligned}$$

In \mathbb{R}_-^3 the above relations hold true if we exchange β with $-\beta$ according to (2.1).

2.2. Equilibrium problem for the interface crack with non-penetration conditions. Consider the composite of two elastic orthotropic materials joined along the plane $x_2 = 0$, which was described in Section 2.1. Assume that in each cross-section with $x_3 = \text{const}$ the solid occupies a domain $\Omega \subset \mathbb{R}^2$ consisting of two sub-domains $\Omega^+ \subset \mathbb{R}_+^2$ and $\Omega^- \subset \mathbb{R}_-^2$ with the interface Σ located on the line $x_2 = 0$. Let Ω be bounded by the Lipschitz boundary $\partial\Omega = \Gamma_N \cup \Gamma_D$ with an outward normal vector $n = (n_1, n_2)^\top$, where $\Gamma_D \neq \emptyset$. We suppose that the crack Γ_C is a part of the interface Σ and define the domain with the crack as $\Omega_C = \Omega \setminus \bar{\Gamma}_C$. Its boundary $\partial\Omega_C$ is the union of Γ_N , Γ_D , and the crack surfaces Γ_C^\pm .

To prevent mutual inter-penetrations between the opposite crack surfaces Γ_C^+ and Γ_C^- we impose a non-negativity condition on the jump of the displacement normal to the crack (u_2 -component), see [12]. Let $g = (g_1, g_2, g_3)^\top$ represent a surface traction given at Γ_N , and, without loss of generality, assume that the volume force is zero. Further, the solid is assumed to be fixed at Γ_D . The problem of equilibrium of the composite with a crack is finally described by the following non-linear (at Γ_C) relations:

$$\begin{aligned}
(2.8) \quad & -\sigma_{1\alpha,\alpha}(u) = -\sigma_{2\alpha,\alpha}(u) = -\sigma_{3\alpha,\alpha}(u) = 0 \quad \text{in } \Omega_C, \\
& \sigma_{12}(u) = \sigma_{23}(u) = 0 \quad \text{on } \Gamma_C^\pm, \\
& \llbracket \sigma_{22}(u) \rrbracket = 0, \llbracket u_2 \rrbracket \geq 0, \sigma_{22}(u) \leq 0, \sigma_{22}(u) \llbracket u_2 \rrbracket = 0 \quad \text{on } \Gamma_C, \\
& \llbracket u_1 \rrbracket = \llbracket u_2 \rrbracket = \llbracket u_3 \rrbracket = 0, \quad \text{on } \Sigma \setminus \Gamma_C, \\
& \llbracket \sigma_{12}(u) \rrbracket = \llbracket \sigma_{22}(u) \rrbracket = \llbracket \sigma_{23}(u) \rrbracket = 0 \\
& \sigma_{1\alpha}(u)n_\alpha = g_1, \sigma_{2\alpha}(u)n_\alpha = g_2, \sigma_{3\alpha}(u)n_\alpha = g_3 \quad \text{on } \Gamma_N, \\
& u_1 = u_2 = u_3 = 0 \quad \text{on } \Gamma_D,
\end{aligned}$$

where the summation convention over repeated indices $\alpha = 1, 2$ is used. Here $\llbracket u \rrbracket = u^+ - u^-$ and $\llbracket \sigma(u) \rrbracket = \sigma^\beta(u^+) - \sigma^{-\beta}(u^-)$ denote the jumps across the interface.

We introduce the cone of admissible displacements which accounts for all the boundary conditions imposed on u in (2.8) as

$$\begin{aligned} K(\Omega_C) &= \{u \in H(\Omega_C) : \llbracket u_2 \rrbracket \geq 0 \text{ on } \Gamma_C\} \text{ with} \\ H(\Omega_C) &= \{u \in H^1(\Omega_C)^3 : u = 0 \text{ on } \Gamma_D\}. \end{aligned}$$

For given $g \in L^2(\Gamma_N)^3$ the potential energy of the composite with a crack is defined by

$$(2.9) \quad \Pi(u) = \frac{1}{2} \int_{\Omega_C} \sigma_{ij}(u) \varepsilon_{ij}(u) dx - \int_{\Gamma_N} g_i u_i ds.$$

The weak solution $u \in K(\Omega_C)$ to the equilibrium problem (2.8) is defined as the solution to the constrained minimization problem

$$(2.10) \quad \text{minimize } \Pi(v) \text{ over } v \in K(\Omega_C).$$

The optimality condition to (2.10) is expressed by the variational inequality

$$(2.11) \quad \int_{\Omega_C} \sigma_{ij}(u) \varepsilon_{ij}(v - u) dx \geq \int_{\Gamma_N} g_i (v - u)_i ds \text{ for all } v \in K(\Omega_C).$$

For unique solvability of (2.10) (or, equivalently (2.11)) uniform positivity of the quadratic term is needed, *i.e.*, the existence of an angle β and a constant $c_0(\beta) > 0$ such that

$$(2.12) \quad \int_{\Omega_C} \sigma_{ij}(u) \varepsilon_{ij}(u) dx \geq c_0(\beta) \|u\|_{H(\Omega_C)}^2 \text{ for every } u \in H(\Omega_C)$$

holds. If the 5×5 -matrix in (2.7) has the minimal eigenvalue $\lambda_{\min}(\beta) > 0$ for some β , in this case, a Korn-type argument implies (2.12).

3. DELAMINATION OF THE COMPOSITE VIA OPTIMIZATION

To describe the delamination between Ω^+ and Ω^- in the model introduced in Section 2, we fix the length l_0 of an initial crack at $t = 0$ and look for its "time"-evolution $l(t) \geq l_0$ with respect to a (loading) parameter $t > 0$. With one crack tip fixed, the length-parameter $l(t)$ determines the position of the second crack tip at $t \geq 0$.

In a natural way we arrive at a one-parameter optimization problem. At every time-step t , the global setting consists of the minimization of an *a priori* given cost functional $T(l)$ (the total potential energy) over all admissible crack lengths $l \geq l_0$. This formulation requires to solve

(2.10) with the crack Γ_C of length l to obtain $T(l)$. Employing the shape (directional) derivative of the cost function at l_0 provides the local optimality condition, which coincides with the Griffith fracture criterion. We combine these two approaches to derive a computationally constructive strategy for optimization.

3.1. Reduced potential energy function and its shape derivative. For $L > 0$ let the crack Γ_C at the interface $\Sigma = \{0 \leq x_1 \leq L, x_2 = 0\}$ be given by the set

$$(3.1) \quad \Gamma_C = \{0 < x_1 < l, \quad x_2 = 0\}, \quad 0 \leq l \leq L.$$

Specifically we assume that the left crack-tip $(0, 0)^\top$ is fixed on the boundary $\partial\Omega$ and the right tip $(l, 0)^\top$ is located at the interface inside Ω . If $l = L$ then the right end of the crack meets $\partial\Omega$.

For the crack (3.1) a reduced potential energy function P depending on the crack-length parameter $l \in [0, L]$ is defined according to (2.9) and (2.10):

$$(3.2) \quad P(l) := \Pi(u) = \min_{v \in K(\Omega_C)} \Pi(v).$$

From (3.2) we deduce that P is a continuous, decreasing, and uniformly bounded function:

$$(3.3) \quad P \in C([0, L]), \quad 0 \geq P(\bar{l}) \geq P(l) \geq P(L) \text{ for } 0 \leq \bar{l} \leq l \leq L.$$

Fix $l \in (0, L)$ and let B_0, B_1 be such that $(l, 0)^\top \in B_1 \subset B_0 \subset \Omega$. Let $\chi \in W^{1,\infty}(\mathbb{R}^2)$ be an arbitrary cut-off function with support in a neighborhood of the crack tip, such that $\chi = 1$ in B_1 and $\chi = 0$ outside of B_0 . For the solution u of (2.10), the shape derivative $P'(l)$ of (3.2) (in direction $(\chi, 0)^\top$) is found to be (see [15]):

$$(3.4) \quad P'(l) = \int_{\Omega_C} \sigma_{ij}(u) \left(\frac{1}{2} \chi_{,1} \varepsilon_{ij}(u) - E_{ij}(\nabla \chi; u) \right) dx,$$

where E denotes a 3×3 -symmetric tensor (with $E_{33} = 0$) of the generalized strain

$$(3.5) \quad \begin{aligned} E_{11}(\nabla \chi; u) &= \chi_{,1} u_{1,1}, & E_{22}(\nabla \chi; u) &= \chi_{,2} u_{2,1}, \\ E_{12}(\nabla \chi; u) &= 0.5(\chi_{,2} u_{1,1} + \chi_{,1} u_{2,1}), \\ E_{23}(\nabla \chi; u) &= 0.5 \chi_{,2} u_{3,1}, & E_{13}(\nabla \chi; u) &= 0.5 \chi_{,1} u_{3,1}. \end{aligned}$$

The value of $-P'(l)$ describes the energy release rate at the vicinity of the crack, and it is independent of χ . In fact, let us integrate by parts (3.4) in $\Omega_C \setminus B_1$, using (2.8) and $\chi = 1$ in B_1 . For an outward normal vector $b = (b_1, b_2)^\top$ at ∂B_1 , an equivalent representation of the

shape derivative by the integral over a closed contour ∂B_1 (see [15]) is obtained:

$$(3.6) \quad P'(l) = \int_{\partial B_1} \sigma_{ij}(u) \left(\frac{1}{2} b_1 \varepsilon_{ij}(u) - E_{ij}(b; u) \right) ds$$

with b_1 and b_2 replacing $\chi_{,1}$ and $\chi_{,2}$ in (3.5). For $\beta = 0$ and $u_3 = \text{const}$ formula (3.6) coincides with the path-independent Cherepanov-Rice integral, which is well-known in fracture mechanics.

From (3.4) and (3.3) we can conclude that

$$(3.7) \quad P' \in C(0, L), \quad P'(l) \leq 0.$$

Let us notice the general fact that for unilaterally constrained crack problems the second derivatives P'' is set-valued.

3.2. Evolutionary problem of optimization. We assume that the loading depends in a linear way on a parameter $t \geq 0$:

$$(3.8) \quad g(t) = tg.$$

In view of the multiplicative property of the static problem (2.11) it follows that $u(t) = tu$ is a solution of the quasi-static problem: Find $u(t) \in K(\Omega_C)$ such that

$$(3.9) \quad \int_{\Omega_C} \sigma_{ij}(u(t)) \varepsilon_{ij}(v - u(t)) dx \geq t \int_{\Gamma_N} g_i(v - u(t))_i ds$$

for all $v \in K(\Omega_C)$.

We arrive at the reduced potential energy function which is quadratic in t :

$$(3.10) \quad P(l)(t) = t^2 P(l), \quad P'(l)(t) = t^2 P'(l).$$

In addition to the potential energy let us introduce the surface energy distributed uniformly at the crack faces Γ_C^\pm ,

$$(3.11) \quad S(l) := \left(\int_{\Gamma_C^+} + \int_{\Gamma_C^-} \right) \frac{1}{2} \gamma ds = \gamma l,$$

where $\gamma > 0$ expresses the material parameter of fracture toughness. The total potential energy T is defined as the sum of P from (3.10) and S from (3.11):

$$(3.12) \quad T(l)(t) := P(l)(t) + S(l) = t^2 P(l) + \gamma l.$$

Let an initial crack with $l_0 \in (0, L)$ be fixed at $t = 0$. To determine an actual state $l(t)$ of the crack for $t > 0$ following the principle of virtual work, we have to minimize the total potential energy over all

admissible cracks. The standard assumption of brittle fracture does not allow the crack to disappear. In this way, from (3.12) we arrive at an optimization problem at every "time" t subject to a constraint $l \geq l_0$:

$$(3.13) \quad \text{minimize } \gamma l + t^2 P(l) \quad \text{over } l \in [l_0, L].$$

Due to the linearity of $S(l)$ and (3.3), the function $T(l)$ is bounded and uniformly continuous in $[0, L]$. Hence there exists a global minimizer $l(t) \in [l_0, L]$ for (3.13) satisfying

$$(3.14) \quad \gamma l(t) + t^2 P(l(t)) \leq \gamma l + t^2 P(l) \quad \text{for all } l \in [l_0, L], \quad t \geq 0.$$

It can be verified (see [5]) that the necessary and sufficient conditions for (3.14) are given by the system:

$$(3.15a) \quad l(0) = l_0,$$

$$(3.15b) \quad l(t) \geq l(s) \quad \text{for } t > s,$$

$$(3.15c) \quad \gamma l(t) + t^2 P(l(t)) \leq \gamma l + t^2 P(l) \quad \text{for all } l \geq l^-(t),$$

$$(3.15d) \quad \gamma l(t) + t^2 P(l(t)) \leq \gamma l(s) + t^2 P(l(s)) \quad \text{for all } s \leq t.$$

Here, we use the notation $l^-(t) = \lim_{s \rightarrow t} l(s)$ for $s < t$, and analogously $l^+(t) = \lim_{s \rightarrow t} l(s)$ for $s > t$. In fact, the initial condition at $t = 0$ implies (3.15a), the model of brittle fracture requires that $l(t)$ should be an increasing function of t as written in (3.15b), and (3.15c)–(3.15d) follow directly from (3.14). In view of (3.7), the differentiability of P and (3.15c) lead to the necessary optimality condition

$$(3.16) \quad \gamma + t^2 P'(l(t)) \geq 0.$$

It is important to note that (3.15d) holds true in the case where l is continuous as well as in the case of a jump $l^+(t) \neq l^-(t)$. The jump can be characterized by

$$(3.17) \quad \gamma[l^+(t) - l^-(t)] + t^2[P(l^+(t)) - P(l^-(t))] = 0.$$

Alternatively, if $l(t)$ were a uniformly continuous function, then $l^+(t) = l^-(t)$ in (3.17) and the Griffith law of fracture would be satisfied:

$$(3.18) \quad \begin{aligned} & l(0) = l_0, \\ & l'(t) \geq 0, \quad \gamma + t^2 P'(l(t)) \geq 0, \quad l'(t)(\gamma + t^2 P'(l(t))) = 0, \quad t \geq 0. \end{aligned}$$

Using non-positivity of P' we define

$$(3.19) \quad G(t, l) := t - \sqrt{\gamma/(-P'(l))}, \quad P'(l) \neq 0$$

and get the set of critical points for (3.13):

$$(3.20) \quad M_t = \begin{cases} L, \\ l_0 & \text{if } G(t, l_0) \leq 0 \text{ or } P'(l_0) = 0, \\ l & \text{if } G(t, l) = 0 \text{ and } l \geq l(s) \text{ for } s \leq t. \end{cases}$$

Further, (3.13) is equivalent to

$$(3.21) \quad \begin{aligned} & l(0) = l_0, \\ & \text{minimize } \gamma l + t^2 P(l) \quad \text{over } l \in M_t \quad \text{for } t > 0. \end{aligned}$$

The advantage of our formulation (3.21) is related to the fact that it not only uses function values $T(l)$ but also the derivatives $T'(l)$ which gives a more accurate account of the extrema. In the numerical realization we find that for (3.13) a finer discretization with respect to l is necessary to achieve the same accuracy as (3.21).

4. NUMERICAL EXAMPLE

4.1. Data for numerical calculations. We choose the following symmetric geometry for the composite with a crack as presented in Figure 1. The domain Ω is chosen to be a square in \mathbb{R}^2 with its boundary

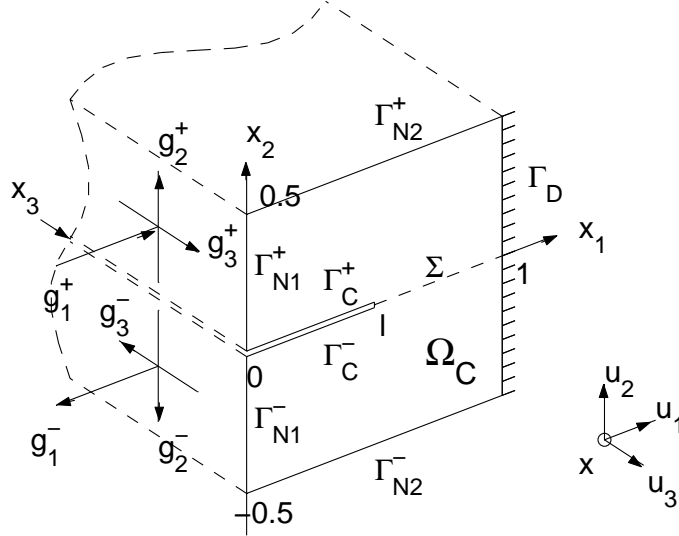


FIGURE 1. Geometry of domain Ω_C .

decomposed as follows:

$$\begin{aligned}\Gamma_D &= \{x_1 = 1, |x_2| \leq 0.5\}, & \Gamma_N &= \Gamma_{N1}^+ \cup \Gamma_{N1}^- \cup \Gamma_{N2}^+ \cup \Gamma_{N2}^-, \\ \Gamma_{N1}^\pm &= \{x_1 = 0, 0 \leq \pm x_2 \leq 0.5\}, & \Gamma_{N2}^\pm &= \{0 < x_1 < 1, x_2 = \pm 0.5\}.\end{aligned}$$

We assume that the crack Γ_C is of length $0 < l < L = 1$. The elastic problem (2.8) in Ω_C is considered with the following boundary conditions imposed on Γ_N :

$$(4.1) \quad \begin{aligned}\sigma_{12}(u) = \sigma_{22}(u) = \sigma_{23}(u) &= 0 & \text{on } \Gamma_{N2}^\pm, \\ -\sigma_{11}(u) = g_1^\pm, \quad -\sigma_{12}(u) = g_2^\pm, \quad -\sigma_{13}(u) = g_3^\pm & \text{on } \Gamma_{N1}^\pm,\end{aligned}$$

where we assume anti-symmetric loading corresponding to mode-3:

$$(4.2) \quad g_3^\pm = \mp g_0, \quad g_1^\pm = g_2^\pm = 0, \quad g_0 = 0.001\mu \approx 3.5376(\text{mPa}),$$

as illustrated in Figure 1.

We utilize the material parameters with the values from [14]:

$$\begin{aligned}E_1 = E_2 = E &= 10160(\text{mPa}), \quad E_3 = 139400(\text{mPa}), \\ G_{31} = G_{32} = G_3 &= 4600(\text{mPa}), \quad G_{21} = \frac{E}{2(1+\nu)} \approx 3537.6(\text{mPa}), \\ \nu_{21} = \nu &= 0.436, \quad \nu_{31} = \nu_{32} = \nu_3 = 0.3.\end{aligned}$$

The corresponding minimal eigenvalues $\lambda_{min}(\beta)$ of the matrix in (2.7) are found to be positive for $\beta \in [-\pi/2, \pi/2]$. They are approximately constant with value $\lambda_{min} \approx 3537.6$. In this case (2.12) holds, and the interface crack problem formulated in Section 2.2 is well-posed.

For calculations, the angle β of fibering is taken at the six points $\beta = 0, \pi/16, \pi/8, \pi/4, 3\pi/8, \pi/2$ in $[0, \pi/2]$. This includes the limit cases of the plane isotropic model with $\beta = 0$, and the plane orthotropic model with $\beta = \pi/2$. Note that for $\beta = \pi/4$ the directions of fibering in Ω_C^+ and Ω_C^- are orthogonal to each other.

4.2. The discrete potential energy and its derivative. Following a common procedure in linear elasticity we utilize linear finite-elements on a triangular mesh constructed in Ω_C , and we use a local refinement in a neighborhood of Σ . Discretization of (2.10) results in a quadratic programming problem subject to constraints associated to the non-penetration condition. The numerical implementation of the semi-smooth Newton method for computing its solution is realized as a primal-dual active-set algorithm, which is described in details in [8, 9, 10]. Realizing this algorithm for our example one gets the following numerical results: the appearance of a mixed mode-1 ($\llbracket u_2 \rrbracket \neq 0$)

with mode-3 ($\llbracket u_3 \rrbracket \neq 0$) crack and contact between opposite crack surfaces under pure mode-3 loading. This situation is related to the 3-dimensional elasticity state and shows the advantage of the spatial model with non-penetration conditions, in contrast to plane isotropic ($\beta = 0$) and orthotropic ($\beta = \pi/2$) models.

Note that there is no contact between the crack surfaces in the remaining interval $\beta \in (-\pi/2, 0)$. This case was investigated in [17] for the linear setting of the problem with the condition $\sigma_{22}(u) = 0$ describing stress-free crack faces Γ_C^\pm .

The reduced potential energy function P and its shape derivative are computed from (2.9) and (3.4). For numerical calculations the cut-off function χ in formula (3.4) is taken piecewise-linear in Ω with $\chi = 1$ around the crack tip, $\chi = 0$ near the external boundary $\partial\Omega$, and symmetrically centered with respect to each crack tip. We approximate the functions P and P' by its discrete values in nodal points $l = 0, h, \dots, 1$, respectively $l = h, 2h, \dots, 1 - h$ for $P'(l)$. The results are depicted in Figure 2 for various fibering angles $\beta = 0, \pi/16, \pi/8, \pi/4, 3\pi/8, \pi/2$. Here mPa stands for mega Pascal.

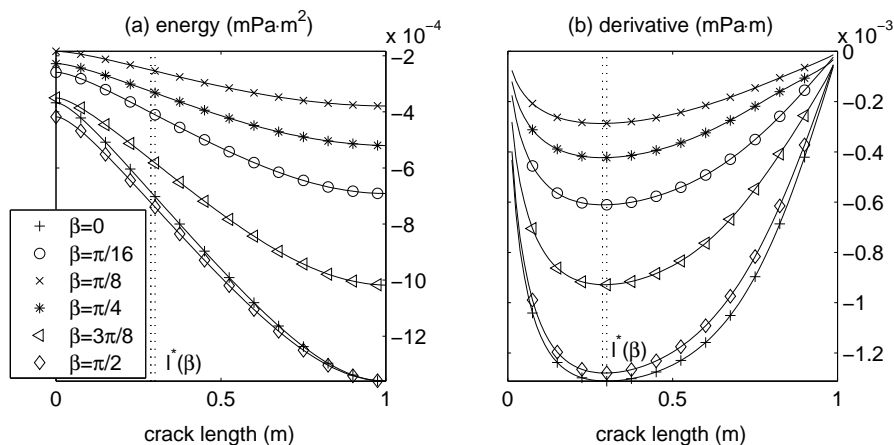


FIGURE 2. Potential energy and its shape derivative.

We find regions of convexity and concavity of P and minima of $P'(l)$:

$$(4.3) \quad P'(l^*) \leq P'(l) \quad \text{for all } l,$$

which occur for $l^* \approx 0.3$ if $\beta \in \{0, \pi/2\}$, and for $l^* \approx 0.2875$ if $\beta \in \{\pi/16, \pi/8, \pi/4, 3\pi/8\}$. They are marked by dotted-lines in Figure 2.

4.3. Delamination under mode-3 loading. For numerical tests the physical parameter γ is taken as $\gamma = 25^2/2\mu \approx 0.011$ (mPa·m).

To endow the loading parameter $t \geq 0$ with a physical scale we multiply it by g_0 and consider the linear loading $g_0 t$ (mPa) according to (3.8). Since $P'(l)$ is negative $G(t, l)$ in (3.19) is well-defined and $g_0 t(l)$ can be obtained from

$$(4.4) \quad 0 = g_0 G(t, l) = g_0 t - g_0 \sqrt{\gamma/(-P'(l))}.$$

For $\beta = \pi/8$ this curve is shown in Figure 3 (a) and (b), respectively, by a dashed-line. In the remainder of this section we analyze the function T defined in (3.12) with respect to local and global minima using (3.18) and (3.21), respectively. The curve defined in (4.4) contains all critical points of T inside the optimization interval.

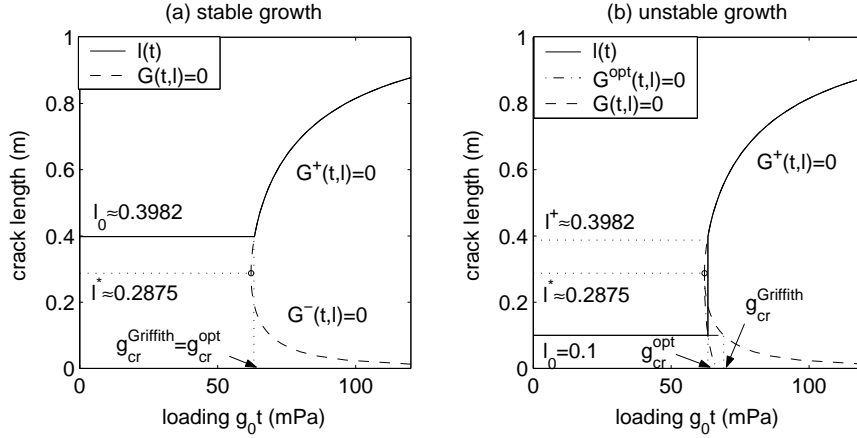


FIGURE 3. Quasi-static crack growth as $\beta = \pi/8$.

We start with the discussion of local minima and fix an arbitrary $l_0 \in (0, 1)$. Following the Griffith fracture hypothesis, a critical loading required to start the growth of a crack of length l_0 is determined from (4.4) by

$$(4.5) \quad g_{\text{cr}}^{\text{Griffith}}(l_0) := g_0 t(l_0) \quad \text{where } G(t(l_0), l_0) = 0.$$

Then the constant function $l(t) = l_0$ is the unique solution to (3.18) as long as $G(t, l_0) < 0$.

Next we seek for the solution $l(t)$ to (3.18) for t such that $G(t, l_0) \geq 0$. For this purpose points $l^* \in (0, 1)$ of local extrema of $t(l)$ must be found. For our data we obtain one minimizer l^* which is equivalently characterized by

$$(4.6) \quad G(t, l^*) \geq G(t, l) \quad \text{for all } l,$$

independently of t . For $\beta = \pi/8$ we obtain $l^* \approx 0.2875$, which is marked with a dotted-line in Figure 3. The line $l = l^*$ separates $G(t, l) = 0$ into two branches along which $l(t)$ is invertible. These two branches are given by $G^-(t, l) = 0$ for $l \in (0, l^*)$, and $G^+(t, l) = 0$ for $l \in [l^*, 1)$. The local solution $l(t) = l_0$ of (3.18) meets either $G^-(t, l) = 0$ if $l_0 < l^*$, or $G^+(t, l) = 0$ if $l_0 \geq l^*$. In the latter case $l(t)$ is an increasing function. Therefore if $l_0 \in [l^*, 1)$, then $l(t)$ satisfying $G^+(t, l(t)) = 0$ is the unique continuous solution to (3.18) for all t . Alternatively, $l(t)$ obtained from $G^-(t, l) = 0$ is a decreasing function. Hence if $l_0 \in (0, l^*)$ then there is no solution $l(t)$ to (3.18), which is continuous at the points $t(l_0)$ satisfying $G(t, l_0) = 0$.

To explain the non-existence of a solution to (3.18) we observe that this relation constitutes a local optimality criterion for (3.13). In our example this results in the following: The points l^* found by (4.3) and (4.6) coincide. Thus $P(l)$ (and hence the total energy $\gamma l + t^2 P(l)$) is convex along the branch $G^+(t, l) = 0$ and concave along $G^-(t, l) = 0$. Hence, points $l(t)$ located on $G^+(t, l) = 0$ provide minima of the total potential energy, whereas points on $G^-(t, l) = 0$ give its local maxima.

Now we look for a global minimizer of the optimization problem (3.14) represented in the form (3.21). Solving it numerically we find continuous solutions for initial cracks of the length $l_0 \in [l^*, 1)$, which coincide with those obtained by the Griffith fracture law (3.18). For $\beta = \pi/8$ and $l_0 \approx 0.3982$ the solution $l(t)$ to (3.20), (3.21) is depicted in Figure 3 (a) with a solid-line. For initial cracks of the length $l_0 \in (0, l^*)$ we derive discontinuous solutions with a jump $l^+ - l_0 > 0$ at the point t where the jump condition (3.17) is satisfied, *i.e.*

$$(4.7) \quad \begin{aligned} g_{\text{cr}}^{\text{opt}}(l_0) &:= g_0 t \text{ where } t \text{ satisfies} \\ G(t, l^+) &= 0, \quad \text{and} \quad \gamma[l^+ - l_0] + t^2[P(l^+) - P(l_0)] = 0. \end{aligned}$$

For $\beta = \pi/8$ and $l_0 = 0.1$ the solution $l(t)$ to (3.20), (3.21) is depicted in Figure 3 (b) with a solid-line. We find numerically that $l^+ \approx 0.3982$ (this value for l_0 was chosen in the previous example of stable propagation), $g_{\text{cr}}^{\text{opt}} \approx 63$ (mPa) and $g_{\text{cr}}^{\text{Griffith}} \approx 69$ (mPa). Here the value of critical loading obtained by the optimization approach from (4.7) is smaller than the one predicted by the Griffith fracture criterion (4.5).

We obtain an improved curve of critical loading by determining $t(l)$ from the following equation

$$(4.8) \quad 0 = G^{\text{opt}}(t, l) := \begin{cases} G^+(t, l) & \text{for } l \in [l^*, 1), \\ g_0 t - g_{\text{cr}}^{\text{opt}}(l) & \text{for } l \in (0, l^*), \end{cases}$$

where $g_{\text{cr}}^{\text{opt}}(l)$ is computed according to (4.7) using (3.21) and (3.20) for all discrete length-parameters $l \in (0, l^*)$. For $\beta = \pi/8$ this curve is depicted in Figure 3 (b) with a dash-dotted line.

The delamination of the composite with the initial crack of length $l_0 \in (0, 1)$ under linear quasi-static loading $g_0 t$ can be constructed geometrically by the following algorithm.

Algorithm 1.

- (0) Fix the initial crack length $l_0 \in (0, 1)$, find $t(l_0)$ such that $G^{\text{opt}}(t(l_0), l_0) = 0$.
- (1) For all $t < t(l_0)$ we have $l(t) = l_0$ (no growth).
- (2) At $t = t(l_0)$ find $l(t) = \max\{l_0, l^+\}$, such that l^+ satisfies $G^{\text{opt}}(t(l_0), l^+) = 0$ (initiation of crack growth).
- (3) For all $t > t(l_0)$ find $l(t)$ such that $G^+(t, l(t)) = 0$ (crack growth).

If $l^+ = l_0$ in Step 2 then the propagating crack is stable and it grows in a continuous way. Otherwise, if $l^+ > l_0$ then the crack propagation is unstable with the jump $l^+ - l_0$.

Next we solve $G^{\text{opt}}(t, l) = 0$ for various choices for the fibering angle $\beta = 0, \pi/16, \pi/8, \pi/4, 3\pi/8, \pi/2$. The results are depicted in Figure 4, and are compared to the solutions of $G(t, l) = 0$ according to the Griffith law (4.5) indicated by dashed lines. The points $l^*(\beta)$ separating

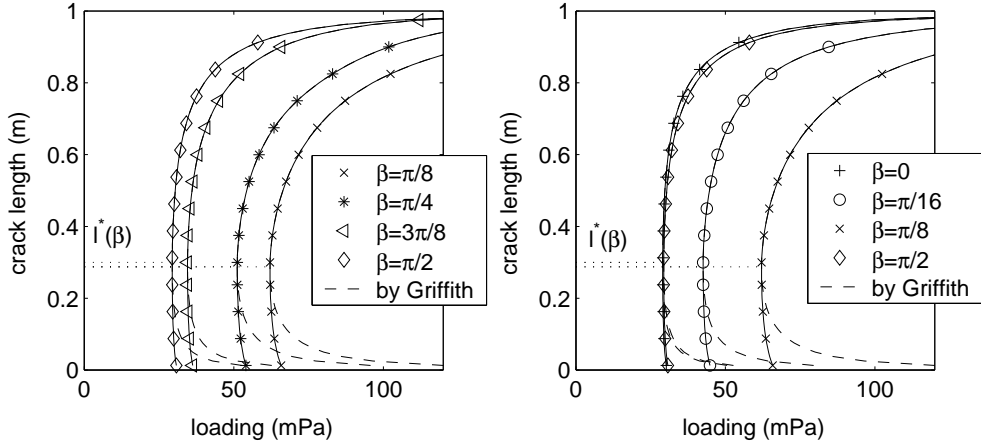


FIGURE 4. Curves $G^{\text{opt}}(t, l) = 0$ of critical loading.

the intervals of stable and unstable crack propagation are indicated by dotted-lines. For every initial crack of length l_0 the delamination process can be constructed by Algorithm 1.

From Figure 4 we can report on the following features:

- The resistance to fracture with respect to the critical mode-3 loading of the composite materials is maximal at $\beta = \pi/8$.
- The curves for the limit cases $\beta = 0$ and $\beta = \pi/2$ are close to each other.
- In the interval $[l^*, 1)$ the crack growth is stable, otherwise it is unstable.

Figure 4 shows clearly that $g_{\text{cr}}^{\text{Griffith}}(l_0) \rightarrow \infty$ as $l_0 \rightarrow 0$. To explain this behavior, note that the limit case $l_0 = 0$ corresponds to the initiation of cracking in a continuous solid which can not be described exactly by the above macro-crack model. Nevertheless, from Figure 4 we may conjecture that $g_{\text{cr}}^{\text{opt}}(0) < \infty$, which is more consistent physically than $g_{\text{cr}}^{\text{Griffith}}(0) = \infty$. The other limit behavior $g_{\text{cr}}^{\text{opt}}(l_0) = g_{\text{cr}}^{\text{Griffith}}(l_0) \rightarrow \infty$ as $l_0 \rightarrow 1$ is due to the boundary condition describing a clamped edge at $l = 1$.

Acknowledgment. The research results were obtained with the support of the Austrian Science Fund (FWF) in the framework of the SFB project F003 "Optimierung und Kontrolle", and the Russian Foundation for Basic Research (03-01-00124).

REFERENCES

- [1] M. Bach, S.A. Nazarov and W.L. Wendland, Stable propagation of a mode-1 planar crack in an anisotropic elastic space. Comparison of the Irwin and the Griffith approaches, *Current Problems Anal. Math. Phys. (Taormina, 1998)*, 167–189, Aracne, Rome, 2000.
- [2] F. Bilteryst and J.-J. Marigo, An energy based analysis of the pull-out problem, *Eur. J. Mech. A/Solids* **22** (2003), 55–69.
- [3] E.G. Cherepanov, *Mechanics of Brittle Fracture*, McGraw-Hill, 1979.
- [4] G. Dal Maso and R. Toader, A model for the quasistatic growth of brittle fractures: Existence and approximation results, *Arch. Rational Mech. Anal.* **162** (2002), 101–135.
- [5] G.A. Francfort and J.-J. Marigo, Revisiting brittle fracture as an energy minimization problem, *J. Mech. Phys. Solids* **46** (1998), 1319–1342.
- [6] A. Friedman and Y. Liu, Propagation of cracks in elastic media, *Arch. Rat. Mech. Anal.* **136** (1996), 235–290.
- [7] M. Hintermüller, K. Ito and K. Kunisch, The primal-dual active set strategy as a semismooth Newton method, *SIAM J. Optim.* **13** (2003), 865–888.
- [8] M. Hintermüller, V.A. Kovtunenکو and K. Kunisch, The primal-dual active set method for a crack problem with non-penetration, *IMA J. Appl. Math.* **69** (2004), 1–26.
- [9] M. Hintermüller, V.A. Kovtunenکو and K. Kunisch, Semismooth Newton methods for a class of unilaterally constrained variational problems, *Adv. Math. Sci. Appl.* **14** (2004), 513–535.

- [10] M. Hintermüller, V.A. Kovtunenکو and K. Kunisch, Generalized Newton methods for crack problems with non-penetration condition, *Numer. Methods Partial Differential Equations*, to appear.
- [11] K. Ito and K. Kunisch, Semi-smooth Newton methods for the variational inequalities of the first kind, *ESAIM, Math. Modelling Numer. Anal.* **37** (2003), 41–62.
- [12] A.M. Khludnev and V.A. Kovtunenکو, *Analysis of Cracks in Solids*, WIT-Press, Southampton, Boston, 2000.
- [13] A.M. Khludnev and J. Sokolowski, The Griffith formula and the Cherepanov-Rice integral for crack problems with unilateral conditions in nonsmooth domains, *Euro. J. Appl. Math.* **10** (1999), 379–394.
- [14] M. König, R. Krüger, K. Kussmaul, M. von Alberti, and M. Gädke, Characterizing static and fatigue interlaminar fracture behavior of a first generation graphite/epoxy composite, *13th Composite Materials: Testing and Design* **13**, *ASTM STP 1242*, J.S. Hooper (Ed.), ASTM, 1997, 60–81.
- [15] V.A. Kovtunenکو, Invariant energy integrals for the non-linear crack problem with possible contact of the crack surfaces, *J. Appl. Maths. Mechs.* **67** (2003), 99–110.
- [16] V.A. Kovtunenکو, Numerical simulation of the non-linear crack problem with non-penetration, *Math. Meth. Appl. Sci.* **27** (2003), 163–179.
- [17] V.A. Kovtunenکو, Interface cracks in composite orthotropic materials and their delamination via global shape optimization, Preprint.
- [18] S.G. Lekhnitskii, *Theory of Elasticity of an Anisotropic Body*, Holden-Day, San Francisco, 1963.
- [19] N. Moës, J. Dolbow and T. Belytschko, A finite element method for crack growth without remeshing, *Int. J. Numer. Math. Engng.* **46** (1999), 131–150.
- [20] N.F. Morozov, *Mathematical Foundation of the Crack Theory*, Nauka, Moscow, 1984, in Russian.
- [21] R. Byron Pipes and N.J. Pagano, Interlaminar stresses in composite laminates under uniform axial extension, *J. Composite Materials* **4** (1970), 538–548.
- [22] J.R. Rice, Elastic fracture mechanics concepts for interfacial cracks, *Trans. ASME. Ser. E. J. Appl. Mech.* **55** (1988), 98–103.
- [23] N. Sukumar, N. Moës, B. Moran and T. Belytschko, Extended finite element method for three-dimensional crack modelling, *Int. J. Numer. Math. Engng.* **48** (2000), 1549–1570.